

Modelling the effect of insulin on the disposal of meal-attributable glucose in type 1 diabetes

Fernando García-García · Roman Hovorka · Malgorzata E. Wilinska · Daniela Elleri · M. Elena Hernando

Abstract The management of postprandial glucose excursions in type 1 diabetes has a major impact on overall glycaemic control. In this work, we propose and evaluate various mechanistic models to characterize the disposal of meal-attributable glucose. Sixteen young volunteers with type 1 diabetes were subject to a variable-target clamp which replicated glucose profiles observed after a high-glycaemic-load ($n = 8$) or a low-glycaemic-load ($n = 8$) evening meal. $[6,6\text{-}^2\text{H}_2]$ and $[\text{U}\text{-}^{13}\text{C};1,2,3,4,5,6,6\text{-}^2\text{H}_7]$ glucose tracers were infused to, respectively, mimic: (a) the expected post-meal suppression of endogenous glucose production and (b) the appearance of glucose due to a standard meal. Six compartmental models (all *a priori* identifiable) were proposed to investigate the remote effect of circulating plasma insulin on the disposal of those glucose tracers from the non-accessible compartments, representing e.g. interstitium. An iterative population-based parameter fitting was employed. Models were evaluated attending to physiological plausibility, posterior identifiability of their

parameter estimates, accuracy—via weighted fitting residuals—and information criteria (i.e. parsimony). The most plausible model, best representing our experimental data, comprised: (1) a remote effect x of insulin active above a threshold $x_C = 1.74 (0.81\text{--}2.50) \cdot 10^{-2} \text{ min}^{-1}$ [median (inter-quartile range)], with parameter x_C having a satisfactory support: coefficient of variation $\text{CV} = 42.33 (31.34\text{--}65.34) \%$, and (2) steady-state conditions at the onset of the experiment ($t = 0$) for the compartment representing the remote effect, but not for the masses of the tracer that mimicked endogenous glucose production. Consequently, our mechanistic model suggests non-homogeneous changes in the disposal rates for meal-attributable glucose in relation to plasma insulin. The model can be applied to the *in silico* simulation of meals for the optimization of postprandial insulin infusion regimes in type 1 diabetes.

Keywords Compartmental model · Glucose disposal · Glucose tracer · Mass balance · Parameter estimation · Type 1 diabetes

1 Introduction

Meals are the most prominent cause of major glycaemic excursions in type 1 diabetes (T1D). For this reason, patients persistently need to make decisions about their prandial insulin boluses, aiming to constrain glucose rises after meals while minimizing their risk of postprandial hyper- and/or hypoglycaemia episodes. Not in vain, these events have a notable impact on overall glycaemic control, as reflected by glycated haemoglobin HbA_{1c} [4]. However, even experienced patients often estimate insulin amounts and/or timing inappropriately [2]. To alleviate this, management strategies beyond carbohydrate counting [18] and

bolus calculators [31] require mechanistic knowledge about the absorption and disposal regimes of meal-attributable glucose.

Various works in the literature have addressed the characterization of postprandial glucose absorption patterns for healthy (i.e. non-T1D) individuals after ingesting either glucose [7, 8, 23] or standard meals: bread or pasta [20, 26, 27]. Notably, a work by Elleri et al. [9] studied for the first time meal absorption in T1D patients who had consumed common mixed meals with complex carbohydrates (CHO), as their dynamics may differ from simpler forms of glucose. The aim of that study was twofold: (1) to obtain mechanistic information applicable to postprandial glycaemia management and (2) to contribute to the field of overnight closed-loop control in T1D. In brief, authors reported that the absorption rate for meal-related glucose ($R_{a,meal}$) reached its maximum at higher values and later times for meals with high-glycaemic-load (HG) than for low-glycaemic-load (LG) meals. Differences were also found in plasma glucose profiles, whereas comparable increases occurred over the first 30 min after both meal types; nonetheless, glucose concentrations after HG peaked at higher levels than for LG and then declined to basal range within 5–6 h. On the contrary, after LG glucose continued to rise progressively and did not return to basal range within 8 h.

Employing data obtained from the clinical study in [9], this work proposes and evaluates different mathematical models to characterize the influence of exogenously administered plasma insulin concentrations on postprandial glucose kinetics in T1D patients. In particular, here we will explore whether different compartmental models, with a compartment representing a remote effect of plasma insulin on glucose disposal, are supported by the experimental data.

2 Methods

2.1 Subjects and experimental protocol

Sixteen young volunteers (seven females and nine males, age range 16–24) diagnosed with T1D for at least 6 months were recruited for a clamp experiment in which prior glycaemic profiles observed after HG or LG evening meals were reproduced. The study was approved by the local ethics committee and participants provided written informed consent.

Subjects were admitted to the Wellcome Trust Clinical Research Facility (Cambridge, UK) on two occasions, separated by one to five weeks. On the preliminary visit, participants consumed either a LG mixed meal (glycaemic load 54, $n = 8$) or a HG meal (glycaemic load 105, $n = 8$) from 18:00 h and over 20 min. Meals were matched for

total CHO: 121 g. Venous blood samples were taken every 10–30 min to determine plasma glucose and insulin. On the subsequent visit, patients were subject to a variable-target glucose clamp adjusting intravenous dextrose infusion rates to reproduce their individual postprandial glucose profiles as measured during the preliminary visit. An adaptive model predictive controller (gMPC version 1.0.2, University of Cambridge, UK) was employed. Participants were admitted after breakfast and fasted from 10:00 to 17:30 h. In this period, intravenous insulin was delivered to obtain stable plasma glucose at 6.0 mmol/L. Starting from 17:30 h (our origin reference time point, i.e. $t = 0$) and until the cessation of the experiment at 02:00 h ($t = 510$ min), intravenous insulin supply consisted of a constant basal delivery plus a variable infusion to mimic the systemic insulin appearance of a subcutaneous bolus of rapid-acting insulin analogue with peak absorption at 50 min [29]. The total amount of insulin was adjusted for each subject's requirements to match 121 g CHO.

In accordance with the aims of Elleri et al.'s experiments [9], [6,6-²H₂] glucose (Cambridge Isotope Laboratories, USA) was infused intravenously in order to trace endogenous glucose production (EGP), starting with a primed constant infusion from 15:30 h ($t = -120$ min), incorporating as well the expected post-meal EGP suppression from 18:00 h ($t = 30$ min). Therefore, [6,6-²H₂] glucose was used as an EGP-mimicking species (onwards abbreviated EM here). In addition, [U-¹³C;1,2,3,4,5,6,6-²H₇] glucose was infused from 18:00 h ($t = 30$ min) to mimic the expected appearance of glucose due to a standard meal; hence it served here as a meal-mimicking tracer (MM). Both infusion patterns were predefined to minimize changes in tracer-to-tracee ratios (TTR) over time, for the sake of accuracy [3, 12].

Blood samples were immediately centrifuged and separated. Plasma glucose was measured with an YSI2300 STAT Plus Analyser (YSI, UK). Tracer-to-tracee ratios (TTR) were calculated using the procedures described by Hovorka et al. [14, 15] to correct for recycled glucose and spectra overlap [21]. A full description of the experimental protocol can be found in [9], as well as detailed absorption and TTR curves. The interested reader is referred to that publication and its online appendices.

2.2 Modelling the kinetics of glucose tracers

We proposed a two-compartmental submodel for each of the infused tracer species: EM and MM, with a common structure between submodels (see Fig. 1, plus Table 1 for nomenclature). The following set of differential equations governs the variation of masses for the EM species, i.e. [6,6-²H₂] glucose:

Table 1 Nomenclature

$g(t)$	Total plasma glucose concentration (mmol/L)
g^0	Initial condition ($t = 0$) for $g(t)$ (mmol/L)
Species EM	EGP-mimicking tracer: [6,6- ² H ₂] glucose
Species MM	Meal absorption-mimicking tracer: [U- ¹³ C;1,2,3,4,5,6,6- ² H ₇] glucose
$g_S(t)$	Plasma concentration of glucose tracer species S (mmol/L)
$q_{1,S}(t), q_{2,S}(t)$	Amount of glucose tracer species S in the accessible ($q_{1,S}$) and non-accessible ($q_{2,S}$) compartments per unit of body weight (μmol/kg)
$q_{1,S}^0, q_{2,S}^0$	Initial conditions ($t = 0$) for $q_{1,S}(t), q_{2,S}(t)$ (μmol/kg)
$u_S(t)$	Appearance rate of tracer species S (μmol/kg min ⁻¹)
u_S^0	Initial condition ($t = 0$) for $u_S(t)$ (μmol/kg min ⁻¹)
TDP	Tracer dilution purity factor (unitless)
V_G	Glucose distribution volume (L/kg)
$F_{01,S}(t)$	Non-insulin-dependent disposal flux of glucose species S (μmol/kg min ⁻¹)
F_{01}	Total non-insulin-dependent glucose disposal flux (μmol/kg min ⁻¹)
$k_{01}(t), k_{02}(t)$	Fractional clearance from the accessible (k_{01}) and non-accessible (k_{02}) compartments (min ⁻¹)
k_{12}, k_{21}	Transfer rate to the accessible from the non-accessible glucose compartment (k_{12}) and vice versa (k_{21}) (min ⁻¹)
k_a	Insulin deactivation rate constant (min ⁻¹)
S_I	Insulin sensitivity (min ⁻¹ per pmol/L)
$i(t)$	Plasma insulin concentration (pmol/L)
i^0	Initial condition ($t = 0$) for $i(t)$ (pmol/L)
$x(t)$	Remote insulin effect (min ⁻¹)
x^0	Initial condition ($t = 0$) for $x(t)$ (min ⁻¹)
x_C	Cut-off value for the activation of $x(t)$ (min ⁻¹)

$$\frac{d}{dt}q_{1,EM}(t) = -[k_{01}(t) + k_{21}]q_{1,EM}(t) + k_{12}q_{2,EM}(t) + u_{EM}(t) \quad (1)$$

$$\frac{d}{dt}q_{2,EM}(t) = k_{21}q_{1,EM}(t) - [k_{02}(t) + k_{12}]q_{2,EM}(t) \quad (2)$$

$$q_{1,EM}(t = 0) = q_{1,EM}^0 \quad (3)$$

$$q_{2,EM}(t = 0) = q_{2,EM}^0 \quad (4)$$

including initial conditions as expressed in (3)–(4).

Similarly for MM, i.e. [U-¹³C;1,2,3,4,5,6,6-²H₇] glucose:

$$\begin{aligned} \frac{d}{dt}q_{1,MM}(t) = & -[k_{01}(t) + k_{21}]q_{1,MM}(t) + k_{12}q_{2,MM}(t) \\ & + TDP \cdot u_{MM}(t) \end{aligned} \quad (5)$$

$$\frac{d}{dt}q_{2,MM}(t) = k_{21}q_{1,MM}(t) - [k_{02}(t) + k_{12}]q_{2,MM}(t) \quad (6)$$

$$q_{1,MM}(t = 0) = 0 \quad (7)$$

$$q_{2,MM}(t = 0) = 0 \quad (8)$$

In these models, accessible subcutaneous compartments represent plasma, whereas non-accessible compartments correspond to other tissues which equilibrate slowly with respect to plasma (e.g. interstitium). Tracer masses of each species S in the accessible compartments $q_{1,S}$ were determined via the measured concentration g_S and accounting for the glucose distribution volume V_G :

$$g_S(t) = \frac{q_{1,S}(t)}{V_G} \quad (9)$$

Two aspects distinguish equations for the MM species with respect to the otherwise identical EM model, namely: (a) a multiplicative factor TDP is applied to the tracer infusion rate u_{MM} in (5) in order to account for differences in purity of the tracer dilution, and (b) initial conditions from (7) and (8) are both fixed to a zero value, since the MM tracer started to be infused at $t = 30$ min, replicating the onset of the reproduced meal intake. Hence, except for TDP , all other parameters are shared between the submodels for each species.

In addition, we assumed that the non-insulin-dependent disposal fluxes $F_{01,S}(t)$ from the accessible compartments are proportional to the total glucose flux F_{01} and to the corresponding tracer-to-tracee ratio TTR_S of species S :

$$F_{01,S}(t) = F_{01} \cdot TTR_S = F_{01} \frac{g_S(t)}{g(t)} \quad (10)$$

where (a) total plasma glucose concentration $g(t)$ was determined experimentally and assumed free of measurement error for our modelling purposes and (b) F_{01} represents the total glucose outflow, which we assumed to be constant over time and addressed as a model parameter [15] for each given subject. Making use of (9) and (10), the fractional clearances or disposal rates $k_{01,S}(t)$ from the accessible compartments yield:

$$k_{01,S}(t) := \frac{F_{01,S}(t)}{q_{1,S}(t)} = \frac{F_{01} \frac{g_S(t)}{g(t)}}{g_S(t) V_G} = \frac{F_{01}}{g(t) V_G} \quad (11)$$

regardless of the particular species S .

For the insulin remote effect $x(t)$, a single-compartmental model with initial condition x^0 was proposed:

$$\frac{d}{dt}x(t) = -k_a x(t) + k_a S_I \cdot i(t) \quad (12)$$

$$x(t = 0) = x^0 \quad (13)$$

Magnitude $x(t)$ models the influence of plasma insulin on glucose disposal rates $k_{02}(t)$ from the non-accessible compartments. Here we studied two types of remote effects. First, we proposed an approach in which the disposal rate

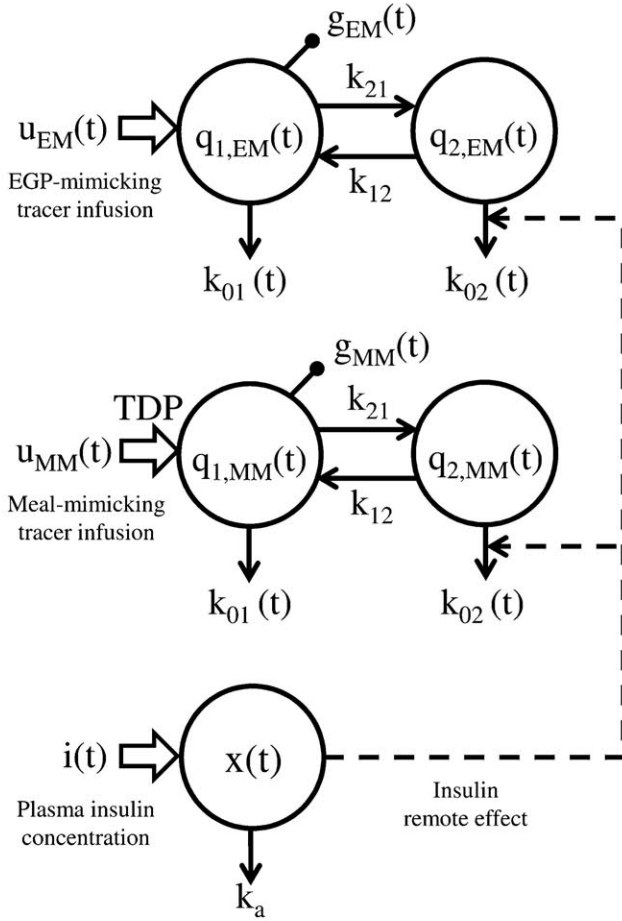


Fig. 1 Schematic of the compartmental models

equals $x(t)$. We will onwards refer to this formulation as “linear”:

$$k_{02}(t) = x(t) \quad (14)$$

Alternatively, we evaluated a second option in which the fractional clearance $k_{02}(t)$ varies proportionately with respect to changes in $x(t)$, but only above a certain threshold x_C , whereas the disposal is suppressed below that value x_C :

$$k_{02}(t) = \begin{cases} x(t) - x_C & \text{if } x(t) - x_C \geq 0 \\ 0 & \text{otherwise} \end{cases} \quad (15)$$

or using an equivalent formulation for compactness:

$$k_{02}(t) = R[x(t) - x_C] \quad (16)$$

where $R[\cdot]$ denotes the ramp function. We will refer to this as a “cut-off” behaviour.

In addition, we investigated the suitability of different forms of initial conditions for (3), (4) and (13). First, an assumption of steady-state conditions for $x(t)$ at $t = 0$ imposes:

$$\frac{d}{dt}x(t=0) = 0 \Rightarrow x^0 = S_I i^0 \quad (17)$$

where i^0 is the insulin concentration measured experimentally at start time ($t = 0$) and S_I represents insulin sensitivity to glucose tracers disposal (Table 1). For the “linear” remote effect, the disposal rate $k_{02}(t)$ from the non-accessible compartments at time $t = 0$ would be equal to:

$$k_{02}(t=0) = x^0 \quad (18)$$

Correspondingly, for the “cut-off” approach we would obtain:

$$k_{02}(t=0) = R[x^0 - x_C] \quad (19)$$

Steady-state conditions for the masses of the EM tracer compartments can also be solved algebraically:

$$\begin{aligned} & \left. \begin{aligned} \frac{d}{dt}q_{1,EM}(t=0) &= 0 \\ \frac{d}{dt}q_{2,EM}(t=0) &= 0 \end{aligned} \right\} \\ & \Rightarrow \begin{cases} q_{1,EM}^0 = \frac{k_{02}(t=0) + k_{12}}{[k_{02}(t=0) + k_{12}] \left[\frac{F_{01}}{s^0 V_G} + k_{21} \right] - k_{12} k_{21}} u_{EM}^0 \\ q_{2,EM}^0 = \frac{k_{21}}{[k_{02}(t=0) + k_{12}] \left[\frac{F_{01}}{s^0 V_G} + k_{21} \right] - k_{12} k_{21}} u_{EM}^0 \end{cases} \quad (20) \end{aligned}$$

where (a) u_{EM}^0 represents the infusion rate for EM at $t = 0$ as employed in the experiment, (b) g_0 is the total glucose concentration measured at start time and (c) $k_{02}(t=0)$ is obtained either through (18) or (19), whichever is applicable.

As an alternative to the steady-state assumption, we explored the option of considering $q_{1,EM}^0$, $q_{2,EM}^0$ and x^0 as extra model parameters, thus implying that the metabolic system was in a non-steady situation (i.e. $d/dt \neq 0$) at the onset of the experiment ($t = 0$). Furthermore, we investigated a mixed case in which the remote effect of insulin $x(t)$ was assumed in steady-state (hence the initial condition from either (18) or (19) applied), whereas EM masses were not considered steady, thus being $q_{1,EM}^0$, $q_{2,EM}^0$ extra model parameters and Eq. (20) for initial conditions becoming not applicable.

In summary, in this work we explored two different configurations for the remote effect of insulin on glucose disposal—either “linear” (L) or “cut-off” (C)—; along with three alternative assumptions for the initial conditions: “steady-state” (S), as “parameters” (P) or “mixed” (M). Therefore, we evaluated and compared a total of six models, namely LS (linear remote effect, plus steady-state initial conditions); CS (cut-off behaviour, plus steady-state); LM (linear, plus mixed initial conditions); CM (cut-off, plus mixed); LP (linear, plus initial conditions as model parameters); and CP (cut-off, plus parameters).

All six models were *a priori* identifiable, satisfying the sufficient condition for *a priori* identifiability described by Carson et al. [5] in terms of the uniqueness of solution for

the system of parameter equations imposed on successive time derivatives at $t = 0$.

2.3 Parameter estimation

For the purpose of parameter estimation, measurement errors were assumed to be normally distributed with zero mean. Errors associated with the measurement of the EGP-mimicking $[6,6-^2\text{H}_2]$ glucose tracer were modelled as multiplicative with coefficient of variation (CV) equal to 5 % [12]. Correspondingly, errors for the meal-mimicking $[\text{U-}^{13}\text{C};1,2,3,4,5,6,6-^2\text{H}_7]$ glucose tracer were assumed multiplicative with $\text{CV} = 5\%$ for concentrations greater than 0.02 mmol/L or otherwise additive with zero mean and standard deviation 0.001 mmol/L. This additive error was determined empirically and signifies that, at low concentrations, instrumentation has precision independent of the measured value.

Model parameters were estimated by means of an iterative two-stage (ITS) population kinetics analysis [16, 22] using SAAM II software (The Epsilon Group, USA). After a preliminary individual parameter fitting—initialization stage—, ITS population analysis iteratively performed a two-step expectation-maximization procedure: (a) parameter estimation—expectation step—including a Bayesian term which penalizes deviations from the current population mean estimate, weighted by the reciprocal of the within-population variance of parameters [22] and (b) an update of population statistics—Maximization step—for the latest parameter fitting. This iterative procedure was repeated until convergence, which was assumed to occur when consecutive parameter estimates differed by $<1\%$.

2.4 Model identification and validation

Parameter estimates were checked for physiological plausibility against reference parameter ranges obtained from previously validated studies [15]. We assessed the posterior identifiability of each parameter in a given model by means of the accuracy of its estimate, considering by convention that a satisfactory estimate was achieved if the CV was below 75 %, acceptable in the range 75–100 %, and non-identifiable if $\text{CV} > 100\%$. These reference thresholds on CVs are similar to (and even lower than) those employed in other comparable metabolic modelling works, e.g. [7, 29].

Runs tests (one-sample Wald–Wolfowitz) were performed in order to ascertain the randomness of the models' weighted residuals of fitting [28].

2.5 Model selection

We assessed which of the six models best represented our observations based on the principle of parsimony, balancing: (a) the accuracy of the fits to experimental data, assessed via the weighted residual sum of squares, and (b) the number of model parameters. For this purpose, Akaike (AIC) and Bayesian (BIC) information criteria were computed by SAAM II, where models should ideally minimize these AIC and BIC scores.

3 Results

3.1 Experimental data

Baseline characteristics for the two groups were statistically comparable (unpaired t tests for normally distributed

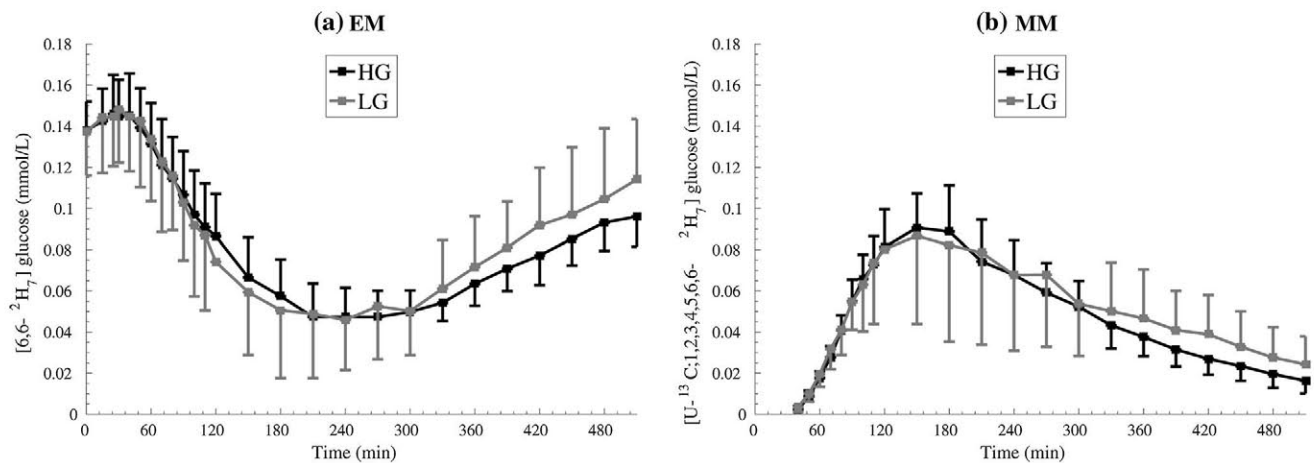


Fig. 2 Plasma tracer concentration profiles in the accessible compartments of the EGP-mimicking tracer (a) and of the meal-mimicking tracer (b), as measured in the variable-target glucose clamp

experiments reproducing a HG or LG evening meal. Values are depicted as mean \pm SD ($n = 8$)

Table 2 Model identification and validation

Model name	Physiological plausibility	Precision of parameter estimates	Runs test	Akaike score (mean \pm SD)	Bayes score (mean \pm SD)
LS	Yes	Satisfactory	31/32	-2.79 ± 2.88	-2.66 ± 2.88
CS	Yes	Satisfactory	31/32	-3.61 ± 0.44	-3.46 ± 0.44
LM	Yes	Satisfactory ^a	31/32	-2.91 ± 2.95	-2.77 ± 2.95
CM	Yes	Satisfactory	32/32	-3.73 ± 0.36	-3.55 ± 0.36
LP	Yes	Satisfactory ^b	31/32	-2.91 ± 2.96	-2.76 ± 2.96
CP	Yes	Satisfactory ^b	32/32	-3.64 ± 0.67	-3.48 ± 0.67

Results

* Fraction of runs tests passed with $p < 0.05$ ($n = 16$ subjects, each with two series of residuals of fitting: for EM and MM)

^a Individual values converged to an identical estimate for one parameter

^b Individual values converged to an identical estimate for two parameters

data, Mann–Whitney and Wilcoxon tests for non-normally distributed data), yielding $p > 0.05$ in all cases [9], namely 3/5 females/males, age 20.8 ± 3.3 years, BMI 24.0 ± 1.5 kg/m², HbA_{1c} 8.7 ± 1.5 %, diabetes duration 7.1 (2.9–20.9) years and total daily insulin 0.8 ± 0.2 U kg^{−1} day^{−1} for the group for which the LG meal was reproduced; versus 4/4 females/males, age 18.1 ± 4.0 years, BMI 22.8 ± 1.2 kg/m², HbA_{1c} 8.7 ± 2.0 %, diabetes duration 7.4 (3.6–11.2) years and total daily insulin 0.9 ± 0.1 U kg^{−1} day^{−1} for the group for which the HG meal was reproduced. Results are expressed as mean \pm SD, except diabetes duration which is as median (inter-quartile range).

Average plasma glucose tracer concentrations in the accessible compartments $g_{EM}(t)$, $g_{MM}(t)$ are depicted in Fig. 2. The variable-target clamp achieved by the adaptive model predictive controller replicated well profiles from the preliminary visit [9].

3.2 Model identification, validation and selection

Table 2 summarizes the results for our model identification and validation procedures. All six models showed physiological plausibility, although two of them—LM and LP—yielded values for the F_{01} parameter (Table 3) in the lower bound of those found by previous validated studies [15]. Posterior identifiability was satisfactory for parameter estimates, with CV < 75 % in all cases (Table 4). However, in three occasions the ITS population fitting resulted in either one parameter (F_{01} for the LM model) or two parameters (F_{01} and x^0 for the LP model; $q_{2,EM}^0$ and x^0 for CP) becoming fixed in their estimation by converging to an identical value for all subjects.

Weighted residuals of model fits are depicted in Fig. 3. In addition to the average residuals obtained at each time point, we computed their root-mean-square (rms) value as a measure of variability across profiles.

Runs tests were applied to the series of weighted residuals. Table 2 presents the fraction of cases that passed the tests, i.e. whenever the null hypothesis of the randomness of residuals could not be rejected with 95 % confidence ($p < 0.05$). Based on the principle of parsimony and accounting for AIC and BIC scores, the model with highest overall *a posteriori* identifiability was CM, hence best representing our experimental data. CM also showed the tightest weighted residuals (both mean and rms, Fig. 3). An example model fit generated by CM is depicted in Fig. 4.

We did not find statistically significant differences ($p < 0.05$) in the values of any of the model parameters for CM across the two subpopulations (HG and LG), neither by independent t tests nor by nonparametric Mann–Whitney tests.

4 Discussion

A number of works in the literature have analysed glucose absorption patterns observed in healthy individuals after ingesting glucose [7, 8, 23] or standard meals [20, 26, 27]. On the basis of one of these studies, Dalla Man et al. [7] generated a model to characterize the absorption of glucose through the gastrointestinal tract and its appearance on circulation, which has been adopted in a number of scenarios, e.g. to model subjects with type 2 diabetes (T2D) [25]. Based on oral glucose tolerance tests (OGTT) ($n = 21$) and data for mixed meals ($n = 20$) obtained from healthy (i.e. non-T1D or T2D) subjects, authors in [7] proposed a three-compartmental model comprising a strongly nonlinear gastric emptying rate which depends on the total amount of glucose in the stomach. In their glucose subsystem, authors described disposal from the non-accessible glucose compartment by means of a Michaelis–Menten relationship, in which its maximum rate V_M (i.e. numerator’s saturation term, according to

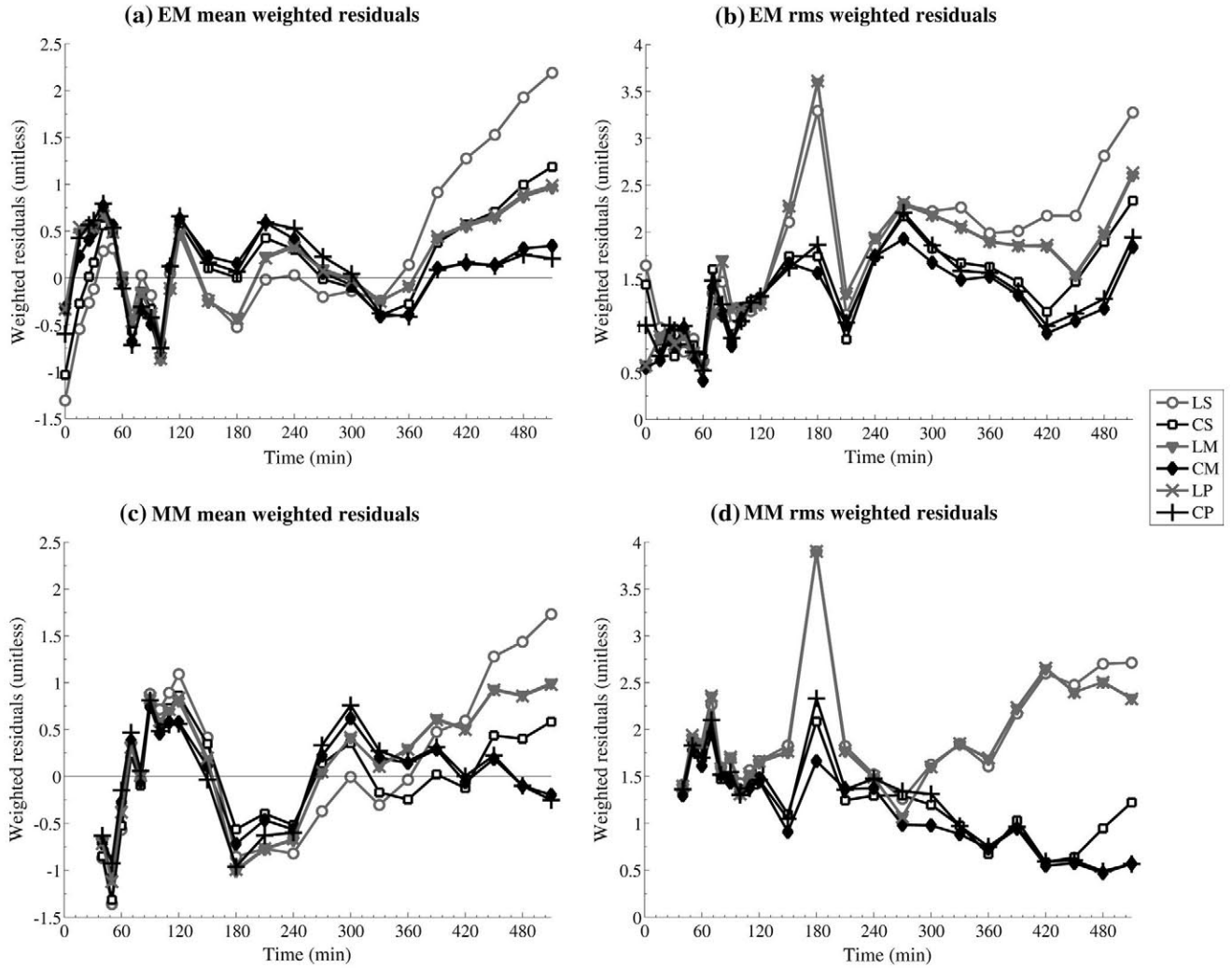


Fig. 3 Mean and root-mean-square (rms) weighted residuals of EM (a, b) and MM (c, d) concentrations for the six models ($n = 16$)

classical Michaelis–Menten nomenclature) is modulated to respond linearly to variations with respect to a remote effect of insulin.

More recently, glucose absorption patterns after mixed meals have been characterized for the first time in T1D patients [9]. That experiment aimed both to: (a) study the mechanistic behaviour of postprandial fluxes and to (b) contribute in the investigation of overnight closed-loop control strategies.

The design of clinical tests for the specific purpose of identifying physiological models can be a challenging task, and model-based design techniques exist to help address model mismatch [10]. However, here we opted for utilizing measurements from Elleri et al.’s work [9] as the source of data for our modelling task, where authors employed a triple-tracer technique in order to estimate glucose appearance in a virtually model-independent manner [3, 12]. Please note that whereas EM and MM tracer profiles

were used here, data from the third tracer: $[U-^{13}C]$ glucose (infused to study meal glucose appearance), were not relevant for the purpose of current work.

Six mathematical models were proposed here to describe the role of exogenously administered plasma insulin on the disposal regimes of meal-attributable glucose, being, to our knowledge, the first proposal to specifically describe the clearance behaviour of meal glucose in T1D patients. Models were compared according to their ability to characterize the remote effect of plasma insulin on the clearance of EGP- and meal-mimicking glucose tracers from non-accessible compartments representing, among other tissues, interstitium. These six nonlinear models comprised mass balance equations for the EM and MM tracer species with a common two-compartmental structure for each, as well as a remote effect $x(t)$ of plasma insulin concentration on the disposal rate $k_{02}(t)$ from the non-accessible compartments with masses $q_{2,s}$. In all models, the non-insulin-dependent disposal flux $F_{01,s}(t)$

Table 3 Parameter estimates for the six models

Model	TDP (10^{-2} unitless)	F_{01} ($\mu\text{mol/kg} \cdot \text{min}^{-1}$)	V_G (10^{-2} L/kg)	S_I (10^{-6}min^{-1} per pmol/L)	k_a (10^{-2}min^{-1})	k_{12} (10^{-2}min^{-1})	k_{21} (10^{-2}min^{-1})	x_C (10^{-2}min^{-1})	$q_{1,EM}^0$ ($\mu\text{mol/kg}$)	$q_{2,EM}^0$ ($\mu\text{mol/kg}$)	x^0 (10^{-2}min^{-1})
LS	85.15 (79.77–91.47)	8.69 (6.51–10.14)	16.22 (12.67–19.07)	38.08 (28.41–56.43)	6.76 (3.02–9.19)	6.76 (2.30–22.07)	8.03 (2.79–19.81)	–	–	–	–
CS	82.26 (77.99–90.46)	11.77 (6.95–13.24)	19.86 (14.17–20.95)	74.25 (41.00–126.55)	4.92 (3.53–8.23)	4.99 (3.11–6.48)	3.16 (1.94–4.40)	0.67 (0.00–1.82)	–	–	–
LM	81.86 (76.78–91.31)	4.04 ^a	18.80 (16.83–20.43)	67.21 (49.13–81.58)	4.81 (2.92–6.69)	3.52 (1.79–14.62)	3.65 (2.63–7.09)	–	26.04 (23.68–29.14)	16.54 (13.24–21.49)	–
CM	79.58 (76.27–87.69)	10.19 (9.02–10.98)	20.14 (16.60–21.74)	135.81 (75.79–211.30)	4.49 (3.89–8.19)	3.19 (2.45–5.14)	2.24 (1.44–3.53)	1.74 (0.81–2.50)	28.00 (23.71–30.78)	15.96 (12.58–19.59)	–
LP	82.11 (76.59–89.36)	4.08 ^a	18.29 (16.70–20.25)	66.57 (45.49–79.85)	5.21 (3.03–6.91)	3.58 (1.96–12.45)	3.65 (2.75–6.77)	–	25.93 (23.02–28.91)	17.17 (13.21–21.05)	0.57 ^a
CP	78.80 (76.02–87.78)	9.24 (7.94–10.91)	19.90 (17.61–21.11)	116.73 (78.64–175.27)	5.48 (3.87–9.47)	2.72 (2.08–4.62)	2.26 (1.57–2.93)	1.57 (0.92–2.06)	27.45 (26.22–30.28)	14.09 ^a	0.50 ^a

Values are expressed as median (inter-quartile range) of individual values ($n = 16$)

^a Individual values converged to an identical estimate

Table 4 Coefficient of variation CV (%) of the parameter estimates

Model	TDP	F_{01}	V_G	S_I	k_a	k_{12}	k_{21}	x_C	$q_{1,EM}^0$	$q_{2,EM}^0$	x^0
LS	2.15 (2.11–2.35)	5.17 (3.25–7.69)	14.20 (6.33–16.71)	15.90 (13.18–20.10)	24.89 (16.93–37.15)	34.56 (27.58–40.76)	36.28 (23.81–47.92)	–	–	–	–
CS	2.37 (2.31–2.70)	12.52 (1.73–17.90)	6.28 (5.24–10.42)	20.92 (15.07–27.29)	26.27 (17.37–35.47)	30.13 (22.83–38.56)	26.36 (17.84–32.57)	42.93 (28.29–63.84)	–	–	–
LM	2.31 (2.17–2.43)	NA	5.26 (4.11–7.77)	14.63 (12.89–20.74)	20.18 (14.62–26.62)	24.22 (21.43–29.47)	11.20 (8.39–21.02)	–	6.69 (5.59–8.85)	22.12 (16.99–26.04)	–
CM	2.46 (2.34–2.68)	19.65 (12.14–25.71)	4.50 (4.11–7.69)	22.91 (18.91–27.94)	23.69 (18.82–28.08)	26.14 (21.83–32.69)	14.83 (13.26–23.41)	42.33 (31.34–65.34)	6.16 (5.49–8.57)	21.00 (15.24–25.68)	–
LP	2.28 (2.20–2.42)	NA	5.29 (4.14–8.551)	14.15 (12.40–19.57)	19.99 (15.36–27.47)	24.85 (20.64–28.88)	12.14 (8.39–23.89)	–	6.73 (5.61–9.41)	22.09 (17.81–26.13)	NA
CP	2.34 (2.28–2.43)	18.64 (11.70–27.97)	4.02 (3.89–4.86)	18.17 (15.56–20.94)	20.92 (13.60–28.49)	19.05 (17.36–25.01)	13.61 (11.02–15.99)	34.67 (24.62–48.82)	4.88 (4.77–5.24)	NA	NA

Values are expressed as median (inter-quartile range) of individual values ($n = 16$)
 NA not available, individual values converged to an identical estimate

from the accessible compartments $q_{1,S}$ was assumed to be proportional to both the total flux F_{01} and the corresponding tracer-to-tracee ratio TTR_S . A dimensionless parameter TDP was incorporated to u_{MM} in order to account for variations in purity of tracer dilutions. Differences among the six models resided in two aspects: (a) whether the disposal rate $k_{02}(t)$ was assumed to be “linear” with the remote effect $x(t)$ of insulin or if, conversely, disposal was activated only above a certain “cut-off” value x_C for $x(t)$ and (b) in the type of initial conditions for the differential equations (steady-state assumed or not). Previous results with triple-tracer techniques in a similar experimental set-up [12] justify our assumption that fractional clearances for both EM and MM tracers could safely be assumed equivalent.

Models were evaluated in terms of their ability to fit experimental data of $n = 16$ young individuals with T1D who underwent a variable-target clamp which replicated glucose profiles observed after LG or HG evening meals. All six models were *a priori* identifiable, fulfilling the sufficient condition stated by Carson et al. [5]. However, *a priori* does not guarantee *a posteriori* identifiability [5] and three models converged to fixed values for certain parameters, an issue which may indicate a failure in *a posteriori* identifiability, with suboptimal fits possibly due to an undesired convergence of the ITS numerical algorithm to local optima. The models which did not suffer from such issue—i.e. LS, CS, CM—showed a satisfactory behaviour regarding *a posteriori* identifiability, with remarkable precision of parameter estimates, as showed by the resulting CVs (Table 4).

Another limitation we found is that for LS, CS, LM and LP models, their average EM weighted residuals (Fig. 3, panel a) took inadequately high values for $t \geq 390$ min, caused by the poor fit achieved for a single individual’s data. Nevertheless, this was the unique profile whose residuals did not pass the corresponding Wald–Wolfowitz runs tests (Table 2). On the other hand, models CM and CP did not suffer from such a drawback. The visible peaks in rms weighted residuals at $t = 180$ min (Fig. 3, panels b, d) are due to the fact that, during the experiments, blood samples at that specific time point could be taken for only 9 out of the 16 subjects.

Regarding model validation, for the assessment of physiological plausibility we encountered the hindrance of having reference values obtained through intravenous glucose tolerance tests (IVGTTs) [15]. Although differences in parameter values might arise on the basis of dissimilar protocols [7], we nonetheless expect that the judgement concerning physiological plausibility should not be misguided on this basis.

In general, the three clearance models with “cut-off” activation behaved better than their corresponding “linear” counterpart. Overall, CM model offered the best fit to

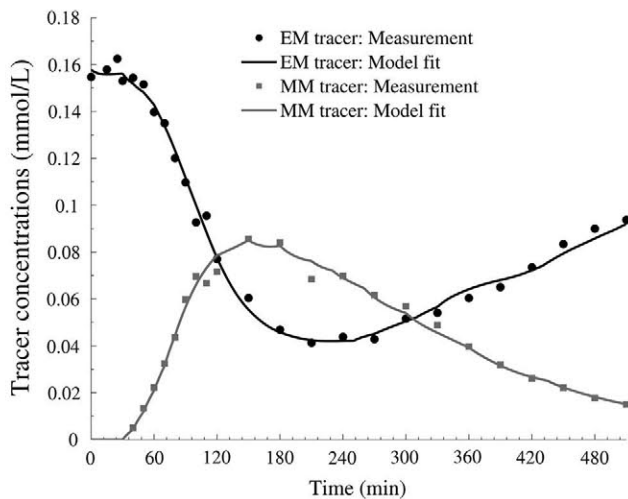


Fig. 4 Example fit by the CM model

data, i.e. with the smallest weighted residuals and the lowest AIC and BIC scores. Its x_C threshold was notably well supported by our data, with $CV = 42.33$ (31.34–65.34) % ($n = 16$) [median (inter-quartile range)]. Furthermore, profiles for both EM and MM tracer concentrations were accurately reconstructed by the CM model, with weighted residuals not showing systematic deviations from randomness: all Wald–Wolfowitz runs tests passed. In addition to the “cut-off” in the remote effect of insulin on disposal, CM comprised steady-state conditions for the compartment $x(t)$ representing this remote effect, but not for the masses of the EM species. This could be originated in the experimental protocol, in which insulin had been infused for 7 h prior to the onset of the clamp, whereas on the contrary the EM tracer had been infused for 2 h [9], and hence, a transient would still be present at $t = 0$. Actually, Fig. 2 (panel a), depicting concentration data, shows EM profiles which are not flat at $t = 0$, but instead peak around $t = 30$ min, a phenomenon which is consistent with the concluded non-stationary situation for $q_{1,EM}(t)$, $q_{2,EM}(t)$.

Due to the experimental complexity of the study, we did not replicate both types of meal for the same population of patients. However, subject features were very similar across populations, with a therefore limited impact on the outcomes.

Concerning applicability, the mechanistic model derived here could be integrated into the *in silico* metabolic simulation of meals [1, 6, 11, 19, 24, 30], in order to optimize postprandial insulin infusion regimes. In addition, those simulations are essential as well for artificial pancreas systems in T1D [17], specially for those based on model predictive control algorithms [13] and therefore relying on physiologically sound models.

5 Conclusion

The role of insulin on the clearance of meal-attributable glucose had not yet been addressed explicitly in the literature. With that aim, this work made use of data obtained from T1D patients during a variable-target glucose clamp, which mimicked the absorption patterns of common mixed meals with complex CHO.

Here we generated various mass balance-based compartmental models and addressed their capability to explain the influence of plasma insulin levels on glucose tracers’ clearance rates. All models were *a priori* identifiable and showed notable precision of the fitted parameter values, in physiological ranges. The selected model CM encompassed a “cut-off” behaviour for the remote effect x of insulin on glucose clearance, as well as initial conditions in a mixed situation: steady state for the insulin compartment, but non-steady for EM tracer masses. CM was capable of explaining experimental observations in a satisfactory, accurate manner.

Compliance with ethical standards

Informed consent Informed consent was obtained from all individual participants included in the study, which was approved by the Addenbrooke’s Hospital (University of Cambridge, UK) ethics committee.

Conflict of interest The authors declare that they have no conflict of interest.

References

1. Abu-Rmieleh A, Garcia-Gabin W, Zambrano D (2010) A robust sliding mode controller with internal model for closed-loop artificial pancreas. *Med Biol Eng Comput* 48(12):1191–1201. doi:10.1007/s11517-010-0665-3
2. Ahola AJ, Mäkimattila S, Saraheimo M, Mikkilä V, Forsblom C, Freese R, Groop P, FinnDIANE Study Group (2010) Many patients with type 1 diabetes estimate their prandial insulin need inappropriately. *J Diabetes* 2(3):194–202. doi:10.1111/j.1753-0407.2010.00086.x
3. Basu R, Di Camillo B, Toffolo G, Basu A, Shah P, Vella A, Rizza R, Cobelli C (2003) Use of a novel triple-tracer approach to assess postprandial glucose metabolism. *Am J Physiol Endocrinol Metab* 284(1):E55–69. doi:10.1152/ajpendo.00190.2001
4. Borg R, Kuenen JC, Carstensen B, Zheng H, Nathan DM, Heine RJ, Nerup J, Borch-Johnsen K, Witte DR, ADAG Study Group (2010) Associations between features of glucose exposure and A1C: the A1C-derived average glucose (ADAG) study. *Diabetes* 59(7):1585–1590. doi:10.2337/db09-1774
5. Carson ER, Cobelli C, Finkelstein L (1983) The mathematical modeling of metabolic and endocrine systems: model formulation, identification, and validation, 1st edn. Wiley, New York
6. Clarke WL, Anderson S, Breton M, Patek S, Kashmer L, Kovatchev B (2009) Closed-loop artificial pancreas using subcutaneous glucose sensing and insulin delivery and a model

- predictive control algorithm: the Virginia experience. *J Diabetes Sci Technol* 3(5):1031–1038
7. Dalla Man C, Camilleri M, Cobelli C (2006) A system model of oral glucose absorption: validation on gold standard data. *IEEE Trans Bio Med Eng* 53(12 Pt 1):2472–2478. doi:[10.1109/TBME.2006.883792](https://doi.org/10.1109/TBME.2006.883792)
8. Dalla Man C, Rizza RA, Cobelli C (2007) Meal simulation model of the glucose-insulin system. *IEEE Trans Bio Med Eng* 54(10):1740–1749. doi:[10.1109/TBME.2007.893506](https://doi.org/10.1109/TBME.2007.893506)
9. Elleri D, Allen JM, Harris J, Kumareswaran K, Nodale M, Leclerathna L, Acerini CL, Haidar A, Wilinska ME, Jackson N, Umpleby AM, Evans ML, Dunger DB, Hovorka R (2013) Absorption patterns of meals containing complex carbohydrates in type 1 diabetes. *Diabetologia* 56(5):1108–1117. doi:[10.1007/s00125-013-2852-x](https://doi.org/10.1007/s00125-013-2852-x)
10. Galvanin F, Barolo M, Macchietto S, Bezzo F (2010) Optimal design of clinical tests for the identification of physiological models of type 1 diabetes in the presence of model mismatch. *Med Biol Eng Comput* 49(3):263–277. doi:[10.1007/s11517-010-0717-8](https://doi.org/10.1007/s11517-010-0717-8)
11. Grosman B, Dassau E, Zisser HC, Jovanovic L, Doyle FJ (2010) Zone model predictive control: a strategy to minimize hyper- and hypoglycemic events. *J Diabetes Sci Technol* 4(4):961–975
12. Haidar A, Elleri D, Allen JM, Harris J, Kumareswaran K, Nodale M, Acerini CL, Wilinska ME, Jackson N, Umpleby AM, Evans ML, Dunger DB, Hovorka R (2012) Validity of triple- and dual-tracer techniques to estimate glucose appearance. *Am J Physiol Endocrinol Metab* 302(12):E1493–E1501. doi:[10.1152/ajpendo.00581.2011](https://doi.org/10.1152/ajpendo.00581.2011)
13. Hovorka R (2011) Closed-loop insulin delivery: from bench to clinical practice. *Nat Rev Endocrinol* 7(7):385–395. doi:[10.1038/nrendo.2011.32](https://doi.org/10.1038/nrendo.2011.32)
14. Hovorka R, Jayatilake H, Rogatsky E, Tomuta V, Hovorka T, Stein DT (2007) Calculating glucose fluxes during meal tolerance test: a new computational approach. *Am J Physiol Endocrinol Metab* 293(2):E610–E619. doi:[10.1152/ajpendo.00546.2006](https://doi.org/10.1152/ajpendo.00546.2006)
15. Hovorka R, Shojaae-Moradie F, Carroll PV, Chassin LJ, Gowrie IJ, Jackson NC, Tudor RS, Umpleby AM, Jones RH (2002) Partitioning glucose distribution/transport, disposal, and endogenous production during IVGTT. *Am J Physiol Endocrinol Metab* 282(5):E992–E1007. doi:[10.1152/ajpendo.00304.2001](https://doi.org/10.1152/ajpendo.00304.2001)
16. Hovorka R, Vicini P (2001) Parameter estimation. In: Carson E, Cobelli C (eds) *Modeling methodology for physiology and medicine*. Academic Press, London, pp 107–151
17. Lanzola G, Toffanin C, Di Palma F, Del Favero S, Magni L, Bellazzi R (2015) Designing an artificial pancreas architecture: the AP@home experience. *Med Biol Eng Comput* 53(12):1271–1283. doi:[10.1007/s11517-014-1231-1](https://doi.org/10.1007/s11517-014-1231-1)
18. Laurenzi A, Bolla AM, Panigoni G, Doria V, Uccellatore A, Peretti E, Saibene A, Galimberti G, Bosi E, Scavini M (2011) Effects of carbohydrate counting on glucose control and quality of life over 24 weeks in adult patients with type 1 diabetes on continuous subcutaneous insulin infusion: a randomized, prospective clinical trial (GIOCAR). *Diabetes Care* 34(4):823–827. doi:[10.2337/dc10-1490](https://doi.org/10.2337/dc10-1490)
19. Magni L, Forgiione M, Toffanin C, Dalla Man C, Kovatchev B, De Nicolao G, Cobelli C (2009) Run-to-run tuning of model predictive control for type 1 diabetes subjects: in silico trial. *J Diabetes Sci Technol* 3(5):1091–1098
20. Priebe MG, Wachtters-Hagedoorn RE, Heimweg JAJ, Small A, Preston T, Elzinga H, Stellaard F, Vonk RJ (2008) An explorative study of in vivo digestive starch characteristics and postprandial glucose kinetics of wholemeal wheat bread. *Eur J Nutr* 47(8):417–423. doi:[10.1007/s00394-008-0743-6](https://doi.org/10.1007/s00394-008-0743-6)
21. Rosenblatt J, Chinkes D, Wolfe M, Wolfe RR (1992) Stable isotope tracer analysis by GC-MS, including quantification of isotope effects. *Am J Physiol* 263(3 Pt 1):E584–E596
22. Steimer JL, Mallet A, Golmard JL, Boisvieux JF (1984) Alternative approaches to estimation of population pharmacokinetic parameters: comparison with the nonlinear mixed-effect model. *Drug Metab Rev* 15(1–2):265–292. doi:[10.3109/03602538409015066](https://doi.org/10.3109/03602538409015066)
23. Toffolo G, Dalla Man C, Cobelli C, Sunehag AL (2008) Glucose fluxes during OGTT in adolescents assessed by a stable isotope triple tracer method. *J Pediatr Endocrinol Metab* 21(1):31–45
24. Turksoy K, Bayrak ES, Quinn L, Littlejohn E, Cinar A (2013) Multivariable adaptive closed-loop control of an artificial pancreas without meal and activity announcement. *Diabetes Technol Ther* 15(5):386–400. doi:[10.1089/dia.2012.0283](https://doi.org/10.1089/dia.2012.0283)
25. Vahidi O, Kwok KE, Gopaluni RB, Knop FK (2015) A comprehensive compartmental model of blood glucose regulation for healthy and type 2 diabetic subjects. *Med Biol Eng Comput*. doi:[10.1007/s11517-015-1406-4](https://doi.org/10.1007/s11517-015-1406-4)
26. Wachtters-Hagedoorn RE, Priebe MG, Heimweg JAJ, Heiner AM, Elzinga H, Stellaard F, Vonk RJ (2007) Low-dose acarbose does not delay digestion of starch but reduces its bioavailability. *Diabet Med* 24(6):600–606. doi:[10.1111/j.1464-5491.2007.02115.x](https://doi.org/10.1111/j.1464-5491.2007.02115.x)
27. Wachtters-Hagedoorn RE, Priebe MG, Heimweg JAJ, Heiner AM, Englyst KN, Holst JJ, Stellaard F, Vonk RJ (2006) The rate of intestinal glucose absorption is correlated with plasma glucose-dependent insulinotropic polypeptide concentrations in healthy men. *J Nutr* 136(6):1511–1516
28. Wald A, Wolfowitz J (1940) On a test whether two samples are from the same population. *Ann Math Stat* 11(2):147–162
29. Wilinska M, Chassin L, Schaller H, Schaupp L, Pieber T, Hovorka R (2005) Insulin kinetics in type-1 diabetes: continuous and bolus delivery of rapid acting insulin. *IEEE Trans Biomed Eng* 52(1):3–12. doi:[10.1109/TBME.2004.839639](https://doi.org/10.1109/TBME.2004.839639)
30. Wilinska ME, Budiman ES, Taub MB, Elleri D, Allen JM, Acerini CL, Dunger DB, Hovorka R (2009) Overnight closed-loop insulin delivery with model predictive control: assessment of hypoglycemia and hyperglycemia risk using simulation studies. *J Diabetes Sci Technol* 3(5):1109–1120
31. Zisser H, Robinson L, Bevier W, Dassau E, Ellingsen C, Doyle FJ, Jovanovic L (2008) Bolus calculator: a review of four ‘smart’ insulin pumps. *Diabetes Technol Ther* 10(6):441–444. doi:[10.1089/dia.2007.0284](https://doi.org/10.1089/dia.2007.0284)